CHAPTER 2: BUCKLING ANALYSIS OF SPACE FRAME USING EXPERIMENTAL AND NUMERICAL TECHNIQUES

In this chapter, the study of the buckling modes and the effective length of bars in steel welded space frames has been carried out experimentally and numerically (*using Abaqus software*). A 3D-model of the under-slung bridge has been used for the experimental and numerical study. The bridge model has been designed in such a way that buckling takes place in the top chords. Effective length for each buckling bar was obtained by experimentation and comparison has been done with the simulated results. For the calculation of effective length using simulated results, the distance between the points of contra-flexure was used. This study provided an insight into the buckling behaviour (*buckling modes and effective length ratio*) of the frame members with the change in the cross-section size of the members connected with the buckling member.

2.1. DETAILS OF THE MODEL

A welded steel frame with steel having young's modulus equal to 211805.7 N/mm^2 has been selected for buckling simulation and experimentation. Dimensions of the frame (shown in Figure 2.1) were such that the total length of the specimen 910 mm; width and height both were 300 mm. It was made-up of all 'square' prismatic cross-sectional bars.

Width of bars *AF, ED, FB* and *EC* was 25 mm; width of bars *AB, CD* and *EF* was 12.7 mm. The model frame has been constructed by connecting two 2D-frames at a spacing of 30 cm (*centre to centre*) by using steel bars having a width of 12.7 mm. Two parallel bars (*BC*) have been selected for expected buckling (*their dimensions were chosen in such a way that BC bars buckle first*). The actual model and weld joints were designed and constructed by using IS 800 (2009).

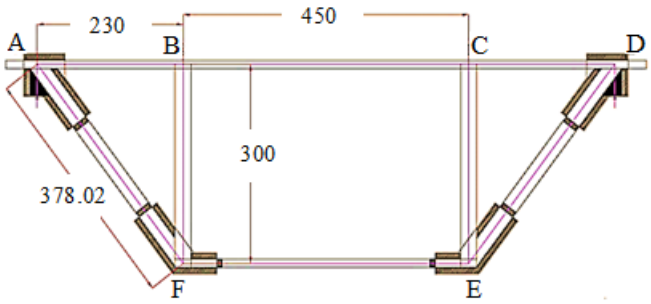

Figure 2.1 Geometry of the frame considered for experimentation (dimensions in mm)

Considered widths of the expected buckling bars BC for two different experiments, were 8mm and 12.7 mm. Point *B* and *C* were selected for the application of vertical point load (*P*). If considering *ABCD* as a single beam, having equal loads at *B* and *C*; zero shear force and equal bending moment would be obtained throughout the length *BC*. For the applied vertical point loads of magnitude '*P*', the buckling load (P_{cr}) in *BC* was $0.77 \times P$.

2.2. METHODOLOGY

Simulations have been conducted on the considered rigid jointed 3D-frame with various square cross-sectional buckling bars with various cross-sections of connecting members using linear perturbation buckling analysis method. Two buckling experiments have been conducted in laboratory for the selected buckling bars (*BC*) in the frame; once having size less than connected members and other with size same as that of connected members. End connections are strengthened by using additional plates. To apply four-point loads an arrangement was constructed such that the loading portal only touches the frame at defined nodes. Simply supported arrangement for the frame was obtained by inserting the slots on both the upper ends of frame into the supporting structures that were firmly attached as shown in Figure 2.2, making the structure similar to an under-slung bridge.

Figure 2.2 Buckling test experimental setup

The buckling modes have been recorded and buckling bars (*BC*) have been scrutinized for finding the effective length of the bars. Basic equation of bending moment (*M*) in terms of deflection (*y*) with respect to *x*-axis can be written as,

$$M = -EI\frac{d^2y}{dx^2} \qquad \text{Equation (2.1)}$$

Where, *EI* is constant throughout the section of buckling bar

The derivative of slope, $\frac{d^2y}{dx^2}$ in the equation of bending moment (Equation 2.1) approximates the curvature. The point of contra-flexure (*M= 0*), can be obtained by using the values of rotation of bar at various sections of the buckling bar (*maxima point of rotation values curve*). Before applying this concept on the simulation results (*for the buckling modes matching with experimental buckling modes*), i.e., the obtained values of the magnitude of the rotation of the expected buckling bars, the method has been cross-verified with classical problem of a column fixed at both ends, for which the effective length ratio obtained was 0.5, as expected. Since the exact buckling behaviour including the shape of actual buckling mode would be quite unpredictable, that is why, in the case of buckling, one can't completely rely only on the conventional methods and concepts.

2.3. RESULTS AND DISCUSSION

The buckling experiment has been conducted for 8 mm and 12.7 mm width size square cross-section bars introduced as bar '*BC*', in the considered frame from which buckling load values were directly obtained and the buckling mode shapes and the effective length of the buckled bars were examined later. Abaqus CAE (2014) has been used for FEM based simulations using linear perturbation analysis method for finding the buckling modes, effective length and the critical load value.

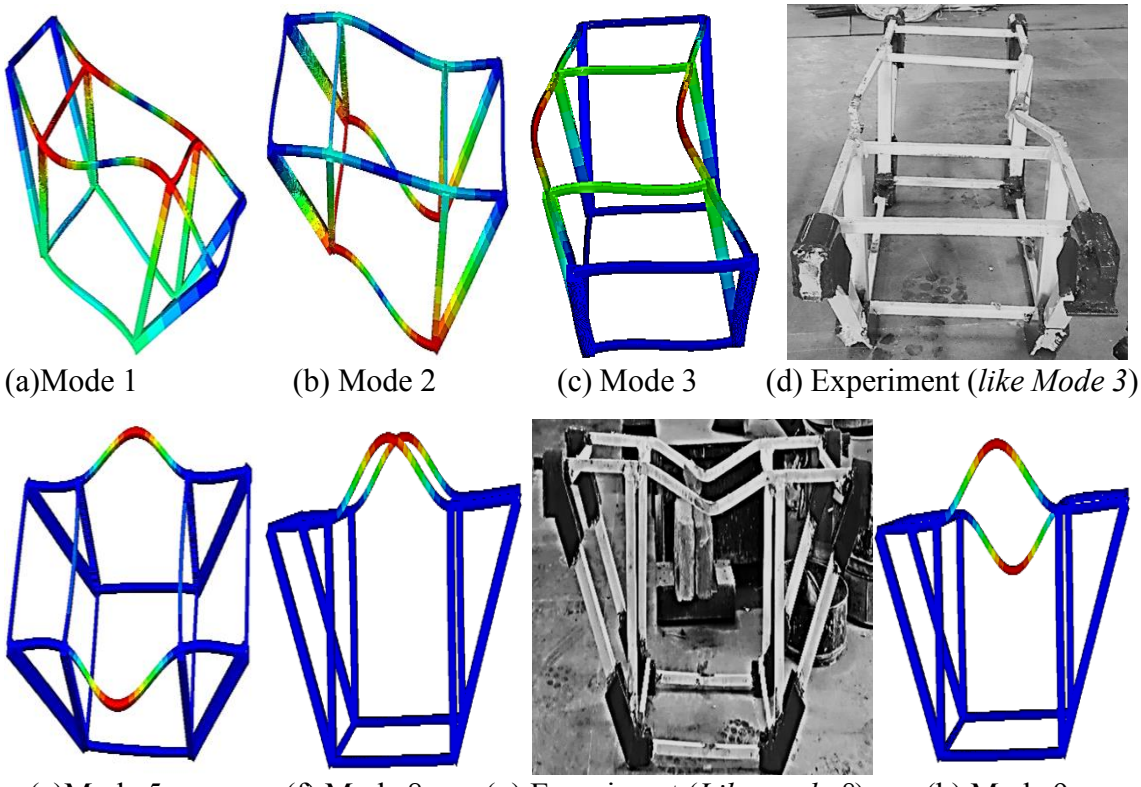

(a)Mode 1 (b) Mode 2 (c) Mode 3 (d) Experiment (*like Mode 3*)

(e)Mode 5 (f) Mode 8 (g) Experiment (*Like mode 8*) (h) Mode 9

Figure 2.3 Mode shapes for 12.7 mm buckling bars

The actual buckling occurred about an axis other than the two conventional axes (*parallel to depth or width of the cross-section)* of the square cross-section in both the experiments. The most expected buckling axis observed in the experimentation was the diagonal axis of the cross-section, for both the different sizes (*8mm and 12 mm*) of the buckling bars.

So, in the observation, the buckling modes obtained by simulation matched with either of the lateral or transverse view of the experimented specimen. In Figure 2.3, for 12.7 mm buckling bars, it can be seen that mode 1 and mode 2 were not obtained in the experiment. Here, mode 3 matched with plan (*lateral*) view of actual failure mode, where one member buckled inward, another buckled outward. Mode 8 matched with elevation (*transverse*) view of actual failure model, where both members buckled in the vertical direction. Here, vertically upward directions in simulation result and downward in the experimental result were considered as same. In simulation, both upward and downward vertical directions of the buckling mode were obtained on varying the mesh size with negligible difference in 'P_{cr}' value but the mode shape obtained after the convergence of 'P_{cr}' value were presented here. Both, mode 3 and mode 8 were asymmetric.

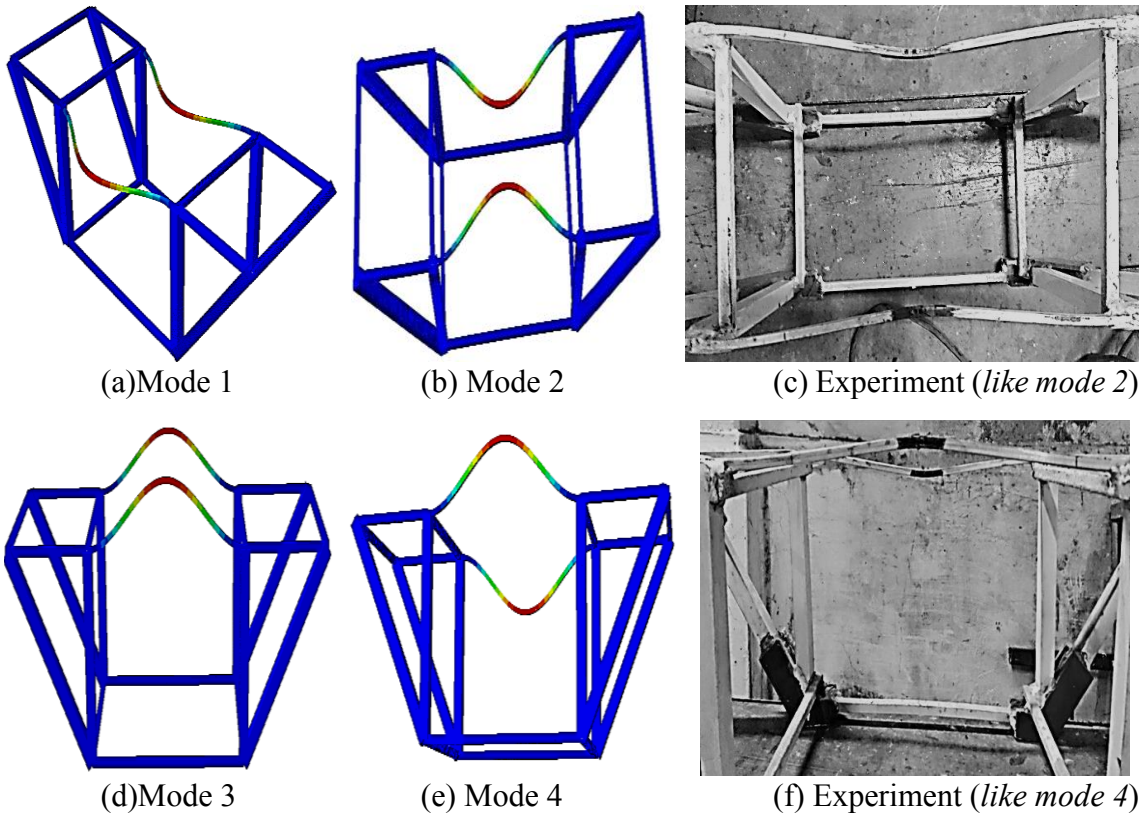

(a)Mode 1 (b) Mode 2 (c) Experiment (*like mode 2*)

(d)Mode 3 (e) Mode 4 (f) Experiment (*like mode 4*)

Figure 2.4 Mode shapes for 8 mm buckling bars

In Figure 2.4, for 8 mm buckling bars, mode 2 matched with the plan (*lateral*) view of actual failure mode, where, both the members buckled inward. Mode 4 matched with elevation (*transverse*) view of actual failure model, where the members bucked upward and other buckled downward. Both mode 2 and mode 4 were symmetric.

Table 2.1 Comparison between experimented and simulated results

Cross-section (*c/s*) of 'BC' bar	**Experimental**			**Simulated**			**Buckling Mode**
	***P* (kN)**	**P_{cr} (kN)**	***K* (±0.2)**	***P* (kN)**	**P_{cr} (kN)**	***K***	
8 mm	19.1	14.7	0.5494	17.8	13.7	0.507	Symmetric
12.7 mm	63.8	40.9	0.6039	72.5	55.8	0.633	Asymmetric

The 'P_{cr}' values obtained by experimentation were closer to the first of the most matching buckling modes obtained by simulation results. Comparison of effective length ratio (*K*) and 'P_{cr}' value between experimental and simulated results have been shown in Table 2.1 for 8 mm and 12.7 mm size buckling bars (*BC*). Buckling mode of 8 mm size bars matched first with the 2nd mode of the simulation results (*in symmetric buckling mode*) and buckling mode of 12.7 mm size bars match with the 3rd mode of the simulation results (*in asymmetric buckling mode*). The results obtained by simulation matched fairly with experimentation results. Because of the differences in the behaviour of buckling modes between experimental and conventional ones (*simulated*), minor variations in results were observed. The experimental 'P_{cr}' value was higher for 8mm bar case and lower for 12.7 mm bar case, in comparison to their corresponding simulation results.

Table 2.2 Simulated results for experimented cases of the buckling member BC

***c/s* of '*BC*' bar**	**Connecting member**	**Combinations based on experimental modes**	
		Modes	**Respective vertical load values, *P* (kN)**
8 mm	12.7 mm	1,3	17.72 (1 in 1 out), 18.20 (both up)
		2 (E),4	17.79 (both in), 18.21 (1 up 1 down)
12.7 mm	12.7 mm	3 (E),8	72.5 (1 in 1 out), 110.4 (both up)
		5,9	95.3 (both out), 110.6 (1 up 1 down)

For the experimented specimens, the simulation results have been produced in Table 2.2. Theoretically (*in simulation*) the very first buckling mode was asymmetric one, so the first row for each buckling bar was of first two asymmetric modes (*corresponding to the experimentally observed asymmetric buckling modes*) and the next row was for symmetric modes (*corresponding to the experimentally observed symmetric buckling modes*). The results similar to experimented ones were denoted with 'E'. It can be seen from the simulated results that the orders of the first matching asymmetric and the symmetric buckling modes for 8 mm size bars were consecutive with nearly equal 'P_{cr}' value. For 12.7 mm bar, there is a noticeable difference in the order of buckling modes.

To extrapolate the results based on the experimental results, simulations were carried out for the frames incorporating buckling bars and connecting bars having cross-section other than those used in the experimentation. Expected modes, '*M*' (*with its order written next to it; like M1 for the very first mode*) were chosen based on experimental observations (*i.e., buckling modes of expected buckling bars* (*BC*) *in both the experiments*). Table comparing effective length ratio, '*K*' and the ratios of the moment of inertia of buckling bar (I_0) with the connecting bar (I), has been constructed as Table 2.3.

Table 2.3 Effective length (L_e) by original length (L) ratio ($L_e/L = K$) and moment of inertia ratio for connecting member (I) by main member (I_0)

***c/s* of '*BC*' bar ↓**	**Connecting member section**							
	8 mm		10 mm		10.08 mm		12.7 mm	
	K	***I/I₀***	***K***	***I/I₀***	***K***	***I/I₀***	***K***	***I/I₀***
8 mm	0.575 (M3)	1	0.520 (M1)	2.44	0.519 (M1)	2.52	0.509 (M1)	6.35
			0.512 (M2)		0.511 (M2)		0.507 (M2)	
10 mm			0.596 (M3)	1	0.591 (M3)	1.03	0.523 (M1)	2.60
							0.520 (M2)	
10.08 mm					0.598 (M3)	1	0.523 (M1)	2.52
							0.520 (M3)	
12.7 mm							0.633 (M3)	1.0

For the 8 mm size buckling bar connected with 10.08 mm size bar and the 10.08 mm buckling bar connected with 12.7 mm size bar, the I/I_0 ratio was same but the effective length ratios were different. Although the higher size bar had higher 'P_{cr}' value for a same I/I_0 ratio with connecting bar but the effective length ratio was lower for the smaller size buckling bar. Same results were observed for the members having I/I_0 ratio as 1.

Table 2.4 Simulation results for main member having 10 mm size square with connecting members of various sizes

***c/s* of *BC* bar**	**Connecting Member**	**Expected Modes**	**P, Load Value (kN)**	**Mode Shape**	***K***	***I/I₀***
10 mm	10 mm	3,5,7,8	31.5 (M3)	1 in 1 out	0.60	1.00
			39.7 (M5)	both in		
	10.08 mm	3,4,7,8	32.1 (M3)	1 in 1 out	0.59	1.03
			39.8 (M4)	both in		
	10.5 mm	3,4,6,7	34.9 (M3)	1 in 1 out	0.57	1.22
			40.1 (M4)	both in		
	11 mm	3,4,5,6	37.3 (M3)	1 in 1 out	0.55	1.46
			40.4 (M4)	both in		
	11.1 mm	2,4,5,6	37.7 (M2)	1 in 1 out	0.54	1.52
			40.5 (M4)	both in		
	11.4 mm	2,3,5,6	38.6 (M2)	1 in 1 out	0.54	1.69
			40.7 (M3)	both in		
	12 mm	2,3,4,5	39.9 (M2)	1 in 1 out	0.530	2.07
			41.1 (M3)	both in	0.520	
	12.5 mm	2,3,4,5	40.6 (M2)	1 in 1 out	0.524	2.44
			41.4 (M3)	both in	0.520	
	12.6 mm	1,3,4,5	40.7 (M1)	1 in 1 out	0.524	2.52
			41.4 (M3)	both in	0.520	
	12.7 mm	1,2,4,5	40.8 (M1)	1 in 1 out	0.523	2.60
			41.5 (M2)	both in	0.520	
	15 mm	1,2,3,4	42.49 (M1)	1 in 1 out	0.510	5.06
			42.51 (M2)	both in	0.510	

In Table 2.4, a fixed cross-sectional size of the buckling bars (*BC*) as 10 mm, and varying cross-sections of the connecting bars were considered. The shapes of expected buckling modes were either like the combination of mode 3 and mode 8 obtained for 12.7 mm deep buckling bar in experiment; or the combination of mode 2 and mode 4 obtained for 8 mm deep buckling bar in experiment. For higher I/I_0 ratio, *K* ratio was lower, i.e., with the use

of a higher size connecting bar the rigidity increased (*for 15 mm connecting bar, K ratio nearly equal to 0.5 was obtained, i.e., the condition of both ends being fully fixed*). As experimentally observed in case of the 8mm cross-sectioned buckling bars connected to 12.7 mm bars; for a 10 mm size buckling bar connected to a 15 mm size buckling bar, an axis of symmetry in the plane of buckling deformation could be expected. As the joint rigidity condition brings *K* ratio close to 0.5, any of the symmetric or asymmetric buckling modes could be expected, as seen for 8 mm cross-sectioned buckling bar case having effective length ratio, $K = 0.509$.

2.4 CONCLUDING REMARKS

With the variation in the cross-section of the buckling member in relation with the cross-section of the connecting members, the buckling modes got affected significantly. Consequently, these variations in the buckling modes influenced the effective length and the critical load. Conclusions have been discussed elaborately in the last chapter, 'SUMMARY AND CONCLUSIONS'.